ENERGY OPTIMISATION OF AIR CONDITIONING SYSTEM USING HYDROSOLAR ROOF AS A HEAT SINK

Lucas M. [a,*], Kaiser A. S. [b], Viedma A. [b], Zamora B. [b]

a Departamento de Ingeniería de Sistemas Industriales
Universidad Miguel Hernández
Avenida de la Universidad, s/n, Edificio "Torreblanca", 03202, Elche, Spain

[b] Departamento de Ingeniería Térmica y de Fluidos
Universidad Politécnica de Cartagena
Campus Muralla del Mar
c/ Dr. Fleming, s/n, 30202, Cartagena, Spain

Abstract

An environmentally friendly alternative device, called Hydrosolar Roof, designed for heat dissipation in buildings has been integrated into a standard air conditioning system. To perform an energy consumption optimisation it has been necessary to include all the elements in a global model. Then, three main subsystems have been considered: Cooling Machine, Hydraulic Network and Hydrosolar Roof. A description of the three subsystems is done and the mathematical model is presented. The Cooling machine thermodynamic model has been carried out using EES (Engineering Equation Solver). The Hydraulic network model has piping, pump and nozzle information. The Hydrosolar Roof direct contact heat and mass transfer simulation has been developed with a CFD code. Special attention has been paid on the cooling efficiency. The global model has been applied to a real prototype facility experimentally tested. All the energy consumptions have been calculated for different pumping heads. A global coefficient of performance (COP) has been defined and the optimum value obtained.

(Keywords: Drop size, Air conditioning, solar chimney, cooling tower, solar energy)

Nomenclature

c_p	Specific heat of water under constant pressure (J/(kg K))
COP	Coefficient of performance
COP_G	Global coefficient of performance
g	Gravity constant (m/s^2)
h	Hydrosolar Roof height (m)
H	Pumping head (m)
H_g	Static head difference (m)
K	Loss coefficient (m/(kg/s)^2)
$\dot{m}_a$	Air mass flow (kg/s)

* Tel: +34 96 6658561, Fax +34 96 6658979. e-mail: mlucas@umh.es

$\dot{m}_w$ Water mass flow (kg/s)

P Pressure (Pa)

$\dot{Q}_{cond}$ Heat dissipated by the Hydrosolar Roof (W)

$\dot{Q}_{evap}$ Cooling load provided by chiller (W)

T_{amb} Ambient temperature (ºC)

T_{cond} Condensation temperature (ºC)

T_{evap} Evaporation temperature (ºC)

T_{dw} Drained water temperature (ºC)

T_{sw} Sprayed water temperature (ºC)

T_{wb} Air wet bulb temperature (ºC)

VMD Volume median diameter (μm)

$\dot{W}_{comp}$ Power consumption of chiller (W)

$\dot{W}_{pump}$ Power consumption of pump (W)

Greek Symbols

ΔT Water temperature reduction (ºC)

$\Delta T_{\max}$ Maximum water temperature reduction (ºC)

η Hydrosolar Roof thermal efficiency

η_{pump} Pump efficiency

1. Introduction

In the summer, energy consumption due to air conditioning is growing world-wide. The main reasons for the increasing demand of energy for air conditioning in buildings during the summer are the higher thermal loads, increasing living standards and occupant comfort demands, as well as buildings' architectural characteristics. Solar driven air conditioning systems are attractive in many regions, due to the fact that cooling demand is generally in phase with insolation. In the last decades, several new activities in this field have started and both research and demonstration projects are carried out in many

countries. Often, in the way of international co-operative projects, for instance, in the framework of the Solar Heating and Cooling Programme of the International Energy Agency (IEA).
An overview of different solar assisted technologies for air conditioning of buildings can be found in Papadopoulos et al., 2003, and Best and Ortega, 1999. Solar assisted cooling systems may be operated by solar thermal collectors connected to thermal driven cooling devices (e.g. absorption, Sözen et al., 2002, or adsorption systems, Alam et al., 2001, and Sumathy et al., 2003); by solar radiation conversion into electricity by photovoltaic cells with the subsequent use of this electricity in a classical motor driven vapour compression chiller; or by solar to mechanical energy converters combined with compression chillers (e.g. solar driven Rankine chiller, Biancardi et al., 1982). Besides, numerous solar concepts have been reported in the literature for reducing building energy consumption to achieve maximum thermal comfort, (see Florides et al., 2002). This paper is located in this last group.

The Hydrosolar Roof is a solar device designed to dissipate heat from water-cooled refrigeration or air conditioning systems, based on the integration of two well-known subsystems: a cooling tower and a solar chimney. This new concept for energy dissipation has been installed in some public buildings in the South of Spain and has been studied in two European Union funded projects (JOE3-CT-7003 and JOR3-CT98-7038). Various global analyses have been performed: Sánchez and Viedma, 2001, developed an experimental study of the first generation Hydrosolar Roof and showed its energy performance; Sánchez et al., 2002, compared the performance of the Hydrosolar Roof with respect to conventional cooling towers and Lucas et al., 2003, optimised the system heat dissipation and changed the Hydrosolar Roof framework design to improve different parameters such as air mass flow and solar radiation, among others.

This paper shows the integration of the Hydrosolar Roof in a whole air conditioning system, including the most important elements from an energy consumption point of view. The optimisation procedure includes a detailed system modelling in order to obtain a minimum energy consumption to produce a given cooling load.

2. System description

A typical centralised air conditioning system (lower part of Figure 1) comprises an indoor air network, a chilled water loop, a cooling machine (chiller) and a condenser water loop. The standard condenser water circuit consists of a chiller condenser, a pump, a cooling tower and a fan. The chiller condenser transfers the indoor cooling load and the heat generated by the compressor into the water circuit. The pump provides the energy to circulate water between the condenser and the cooling tower. The heat is

delivered to the atmosphere by the cooling tower through an evaporative heat transfer process. In this case, the cooling tower is replaced by a new environmentally friendly element, the Hydrosolar Roof.

Figure 1 shows an air conditioning system scheme, with the Hydrosolar Roof as the heat dissipation device in the condenser water circuit. One can also see the different elements mentioned above and the main variables used in the modelling. The Hydrosolar Roof is mounted on the roof of the buildings and is made of a metallic structure and a hydraulic circuit. The structure is composed of a steel framework, which gives support to both the solar collector set and the hydraulic subsystem. The interior space allows air to move across it from bottom to top without obstacles, but it can be considered as being divided into two different zones from a functional point of view. The upper part, known as convection zone, is made up of sloping channels whose walls are solar collector panels. The solar radiation impinges directly or by reflection on these panels increasing their temperature above the ambient level. The air located inside the channels is heated and the natural draft produces an upward air flow. Wind effect increases upward airflow. Therefore, the upper zone is basically a solar chimney at a reduced scale. The lower part, known as the evaporative cooling zone, has a series of nozzles that spray water crosscurrent the upward airflow. The water exchanges mass and energy with the air and is recovered colder. This zone works as a counter-flow cooling tower. The system can be regarded as a two-dimensional solar chimney coupled to a widespread cooling tower. As a standard cooling tower, the Hydrosolar Roof removes heat from the cooling machine's condenser and sends it out to the atmosphere. However, instead of consuming energy to produce the air flow by means of fans, the Hydrosolar Roof generates the buoyancy flow induced by solar and wind energy.

Figure 1

Since the condenser water loop is a main component of HVAC systems, its energy consumption contributes significantly to the overall operating cost. Efficient performance of individual devices as well as the whole condenser water loop have been intensively studied in recent years. Among many published research results, Lu et al., 2004, presented a model-based optimisation strategy for a standard condenser water loop, Soymelez, 2004, developed a thermo-hydraulic approach for estimating the optimum performance point of counter current mechanical draft wet cooling towers, and Cassidy and Stack, 1988, showed that varying the speed of cooling tower fans can reduce its energy consumption at part load conditions. Braun and Doderrich, 1990, proposed a systematic approach to find a near optimal variable speed drive based on parameters estimated from design data. This work applies standard optimisation strategies to an innovative heat dissipation element, named Hydrosolar Roof.

The system's main energy consumptions are located in the cooling machine compressor and the water pump. An optimisation procedure has to consider the effect of the operating parameters on these

consumptions. As the cooling machine is working coupled to the Hydrosolar Roof, a different Hydrosolar Roof performance modifies the cooling machine's working point. At the same time, the water pump sets Hydrosolar Roof performance. In this sense, the three subsystems are closely related. Building up a global model is an essential tool to analyse the interrelations among the different elements and to obtain an optimum performance.

In the first step, it is necessary to identify the operation variables that can be modified and then to know the effect of these modifications. So, the water pumping head at the water Hydrosolar Roof's water condenser circuit is the keystone of the optimisation procedure, but modifying it has different effects in the performance of the components. Considering only the Hydrosolar Roof, modifying the pumping head drives to obtain two opposite effects due to the cooling tower's analogous performance. On the one hand, the higher the pumping head is, the lower the water drop size diameter results and the greater the air-water contact surface obtained, which increases heat dissipation. On the other hand, the higher the pumping head is, the higher the pumped water mass flow, lowering the efficiency due to a higher water/air mass flow ratio. Therefore, dependence between water pumping head and Hydrosolar Roof efficiency is not clear. But it is a certainty that, as a consequence of different water pumping pressures, the Hydrosolar Roof efficiency varies and the water thermal level in the water condenser tank is also modified. This affects the cooling machine condenser's temperature, also, its energy consumption varies.

A global coefficient of performance will be defined as the relation of absorbed energy from the cold region and the consumed energy by the compressor and the pump. This work will show how to optimise energy consumption selecting the pumping head and obtaining for this optimum point the rest of the system parameters.

3. System modelling

A global mathematical model has been developed to achieve a response to the above exposed questions. It includes three main subsystems: *Cooling machine, Hydraulic Network and Hydrosolar Roof.* A description of the three parts is done below. First, the mathematical model of each subsystem is presented and then it is applied to the real case experimentally tested. This is the prototype installed at the Universidad Politécnica de Cartagena (Spain) with a total occupied surface of 36 m^2, and described in Sánchez et al., 2002.

3.1 Cooling machine

The starting value for the cooling machine model is the building cooling load, $\dot{Q}_{evap}$. It depends on several factors, such as building geometry, construction materials or location. However, $\dot{Q}_{evap}$ is considered constant during the optimisation procedure because it is the building's cooling needs, its magnitude is independent from the system efficiency. For the building where the prototype is installed a cooling load of 16 kW was estimated.

Performance of a refrigeration cycle is usually described by a coefficient of performance (*COP*), ASHRAE, 1997. *COP* depends on condensation temperature, T_{cond}, and evaporation temperature, T_{evap}. In this case, taking into account air conditioning application, T_{evap} can also be considered constant, and then *COP* only depends on the higher temperature, T_{cond}. At the same time, T_{cond} depends on the condensing media, water in this case. The energy transferred from the cooling machine to the water is finally rejected by means of heat and mass transfer at the Hydrosolar Roof. So, the thermal level of the water leaving the condenser is the sprayed water temperature, T_{sw}. Condensation temperature is a function of this value, just some degrees above it to allow thermal transfer, $T_{cond} = T_{cond}(T_{sw})$. This is the link the between chiller model (air conditioning cooling machine) and the Hydrosolar Roof model. Thus, as $COP = COP(T_{cond})$ and $T_{cond} = T_{cond}(T_{sw})$, the energy supplied by the compressor is related to the Hydrosolar Roof's sprayed water temperature.

$$\dot{W}_{comp} = \frac{\dot{Q}_{evap}}{COP(T_{sw})}. \tag{1}$$

In this way, once $\dot{Q}_{evap}$ is considered constant, the heat to be evacuated in the Hydrosolar Roof is also only dependent on the sprayed water temperature,

$$\dot{Q}_{cond} = \dot{W}_{comp} + \dot{Q}_{evap} = \dot{Q}_{cond}(T_{sw}). \tag{2}$$

The standard air conditioning cooling machine model has been carried out using a quite popular code among thermodynamic scientists and practitioners: EES (Engineering Equations Solver). The condensation temperature will be evaluated with a standard difference between refrigerant and water ($T_{cond}=T_{sw}+5ºC$) as a design criteria, Rapin and Jaquard, 1997. The refrigerant fluid is R-134a and its thermodynamic properties have been obtained using the fundamental equation of state developed by Tillner-Roth and Baehr, 1994. Other cycle parameters are fixed at standard values: useful overheating (4ºC) and useless overheating (3ºC) at the evaporator exit, pressure drops through the suction line (9,800 Pa) and discharge line (19,600 Pa), underheating at the condenser exit (2ºC), mechanical-electrical compressor efficiency (0.92) and isentropic compressor efficiency (0.9). As the evaporator temperature is kept constant (4.5ºC), the COP is correlated with the condensation temperature. Therefore, the computational model supplies the influence of T_{sw} on the cooling machine

COP. Figure 2 shows the evolution of *COP* as a function of sprayed water temperature.

Figure 2

A second order polynomial function, only appropriate in the studied interval, is used to obtain a mathematical expression to be employed at the optimisation procedure.

$$COP = 0.0074 \cdot (T_{sw})^2 - 0.6897 \cdot T_{sw} + 19.3463 \,. \quad (3)$$

3.2 Hydraulic Network

This section presents the main results for the model established for the hydraulic network between the cooling machine and the Hydrosolar Roof, that is, piping, pump and nozzles. The mathematical equations used to describe the performance of these elements only include the variables that are related to the thermal behaviour of the other two subsystems. In this sense, the Hydrosolar Roof is linked to the hydraulic network through the water mass flow rate and sprayed water drop size, and both parameters are determined by the pumping head.

In order to obtain the relationship between water mass flow rate and pumping head, geometrical data, materials and accessories of the whole network were considered. Its well known performance is essentially a parabolic curve characterised by two terms: the static head difference H_g between the liquid levels at the suction and discharge points, at atmospheric pressure, and the term proportional to the square of the flow rate. This last term includes friction losses in pipes and minor losses as well as additional losses due to the spray nozzles. All of these losses are roughly proportional to the square of the flow rate due to turbulent regime, and modelled by the loss coefficient, K. Then, the hydraulic network can be modelled by the following equation,

$$H = H_g + K\dot{m}_w^2 \,, \quad (4)$$

where H is the pumping head.

For the prototype studied, the performance curve of the hydraulic network was obtained, (see Figure 3). The prototype is 3 m over the water tank free surface that feeds the pump, so H_g = 3 m, and K takes a value equal to 8.654 (m/(kg/s)^2).

Figure 3

Since a variable speed drive pump control has been installed; any operation point on the hydraulic

performance curve can be reached. Pumping energy consumption, $\dot{W}_{pump}$, is a result of the pumping head and water mass flow. A typical value of 85% has been considered for the centrifugal pumps efficiency. In this way,

$$W_{pump} = \frac{g \cdot H \cdot \dot{m}_w}{\eta_{pump}} \quad . \tag{5}$$

Apart from mass flow rate variations, the change in pumping head has a clear influence on the size of the water drops generated. This is very important information for the optimisation due to its influence on the evaporation area available between sprayed water and air. This relationship depends on the nozzle type and size, and can be given as a function between Volume Median Diameter (*VMD*) and pumping pressure. Volume Median Diameter is a mean of characterising drop size distribution, following ASTM Standard, 1996. In the prototype built, Flat Spray nozzles with an orifice diameter of 1 mm are installed. The pressure curve as a function of *VMD* is supplied by nozzle manufacturers, see Figure 4. A potential function is used to obtain a mathematical expression of this curve for the optimisation procedure.

$$VMD = 603.5712 P^{-0.4196} \quad . \tag{6}$$

Figure 4

3.3 Hydrosolar Roof

As a widespread cooling tower, the Hydrosolar Roof cools water by a combination of heat and mass transfer. Fundamentals of these physical phenomena were described by Merkel, 1926, and later on by Nottage, 1941. Others authors, like Mohiuddin and Kant, 1996, have contributed with studies about the cooling tower's systematic design.

From the Merkel model, water temperature decrease depends mainly on the incoming air wet-bulb temperature, (T_{wb}). Therefore, the physical limit to the drained water temperature is the ambient web-bulb temperature. The system's thermal efficiency can be defined as the relation between actual water temperature reduction, the one existing between sprayed and drained water, T_{sw}-$T_{dw,}$ and the water temperature's maximum difference, so:

$$\eta = \frac{T_{sw} - T_{dw}}{T_{sw} - T_{wb}} = \frac{\Delta T}{\Delta T_{\max}} \, . \tag{7}$$

The heat dissipated by the Hydrosolar Roof can be expressed as a function of the water mass flow rate and this efficiency coefficient, and is also the energy received by the water from the cooling machine condenser.

$$\dot{Q}_{cond} = \dot{m}_w c_p \Delta T = \dot{m}_w c_p \eta \Delta T_{\max} \quad (8)$$

To know the influence on the Hydrosolar Roof efficiency of the most important parameters, a deep study of the evaporative processes that take place in this extended cooling tower is needed. Previous work, as the experimental correlations from Sánchez et al., 2002, described the influence on the induced air mass flow and on the system efficiency of the environmental variables as solar radiation, wind velocity and dry and wet bulb air temperatures. However, no water drop size effect was considered. Then, a 2D numerical model by using the general-purpose Fluent code, based on a finite volumes procedure, was generated fixing environmental conditions and studying the influence on the efficiency of the thermodynamic (ΔT_{max} and $\dot{m}_w/\dot{m}_a$) and geometric (VMD) selected parameters. With this purpose, 45 cases have been calculated. The model was validated with the experimental data from the prototype tested.

In the model calculations environmental conditions were fixed at T_{amb}=32ºC and T_{wb}=25.6ºC. Solar radiation was modelled, from measurements in the prototype, with a 20ºC gap between channel plates and ambient temperature. The Hydrosolar Roof prototype height is 0.7 m. With the objective of focusing the calculation effort on the evaporation zone and save computational time, wind effect was substituted by a longitudinal depression in the channel outlet corresponding to a typical value of 1 m/s.

Some of the varying parameters, as ΔT_{max} and VMD, could be fixed with the only restriction of being within the expected range. But the mass flow ratio between water and air, $(\dot{m}_w/\dot{m}_a)$, a usual parameter to characterize cooling towers, could only be fixed indirectly. This value was obtained after a numerical solution because air mass flow was a result of the calculations. Given the environmental conditions, in order to force different water and air mass flow ratio, three water mass flow values were fixed ($\dot{m}_w$ =0.555, 1.11 and 1.665 kg/s). In this way, $\dot{m}_w$, ΔT_{max} and VMD are fixed and $\dot{m}_a$,and subsequently $(\dot{m}_w/\dot{m}_a)$, are determined. From the numerical results, $\dot{m}_a$ can be modelled with the following function,

$$\dot{m}_a = 1.335 + 0.273\dot{m}_w - 6.944 \cdot 10^{-4} VMD + 0.698 \cdot 10^{-2} \Delta T_{\max} . \quad (9)$$

As examples of the calculations carried out, the figures below show water temperature evolution and water vapour mass fraction in the air. Figure 5 shows the water temperature evolution from the inlet water temperature at the nozzle to the outlet water temperature on the floor of the building roof. Figure 6 shows the high water concentration in the continuous phase due to evaporation in the sprayed zone.

Figure 5

Figure 6

With Fluent, the water outlet temperature is calculated for each case. Once this value is known, efficiency can be evaluated. Thus, efficiency results are showed in Figures 7 and 8.

Figure 7

Figure 8

Figure 7 shows efficiency at different ΔT_{max} for $(\dot{m}_w/\dot{m}_a)$=1. It can be observed that the smaller the drop size, the higher the efficiency. This is due to the fact that heat and mass transfer surface between water and air is greater. From this figure, the influence of ΔT_{max} on the efficiency can also be deduced. Figure 8 shows the slight inverse relation between efficiency and water mass flow for ΔT_{max} = 5ºC. Numerical results are in accordance with experimental results since the greater the ratio, the lower the efficiency. All the calculated data has been correlated to obtain a useful efficiency function for the optimisation procedure. An expression for thermal efficiency of the Hydrosolar Roof has been obtained . Dimensionless parameters have been selected taking the work of Fisenko et al., 2004, as a reference.

$$\eta = 0.3775 \cdot \left(\frac{h}{VMD \cdot 10^{-3}} \right)^{1.324} \cdot \left(\frac{\dot{m}_w}{\dot{m}_a} \right)^{-0.0174} \cdot \left(\frac{\Delta T_{\max}}{T_{amb}} \right)^{0.178} \quad (10)$$

Due to the fact that both *VMD* and $(\dot{m}_w/\dot{m}_a)$ are only dependent on *H*, and $\Delta T_{\max}$ depends on T_{sw}, it can be concluded for optimization purposes that thermal efficiency of the Hydrosolar Roof is a function of *H* and T_{sw}, so $\eta=\eta\,(H, T_{sw})$.

In order to validate the numerical procedure, a comparison between the efficiency obtained from the numerical model and the experimental value measured in the prototype installed at the Universidad Politécnica de Cartagena (Spain) was made. A detailed explanation of the prototype technical information and tests performed has been reported in Sánchez et al., 2002. Figure 10 shows the efficiency values versus maximum water temperature differences. Both the numerical and the experimental tendencies are mainly equal. Figure 10 presents both numerical and experimental results for the thermal efficiency of the system at different water and air mass flow ratios. These comparisons with experimental data are obtained for water drop size (*VMD*) of 600 μm, estimated prototype conditions and nozzle catalogue information. Differences less than 10.5% between numerical and experimental results are obtained in any case.

Figure 9

Figure 10

4. Optimisation and discussion

Once the three subsystems have been modelled, it is necessary to link them. Attending to all the equations presented, it is suitable to set out a resolution procedure. From Eq. (8) the energy received by the water from the cooling machine condenser depends on $\dot{m}_w$, η, and ΔT_{max}. The hydraulic network model has showed that $\dot{m}_w$ can be expressed as a function of the pumping head. Considering a constant wet bulb temperature, ΔT_{max} only depends on T_{sw}. At the same time, as a consequence of the results obtained in the numerical calculations, it has been deduced that efficiency, η, depends on T_{sw} and the pumping head, H. In this way, heat dissipated by the Hydrosolar Roof only depends on T_{sw} and H. At the same time, from Eq. (2), the heat released by the cooling machine's condenser is expressed as a function of T_{sw}. As both magnitudes are the same, a single equation with two unknowns, H and T_{sw}, can be obtained. When the pumping head is fixed, T_{sw}, and from it all the rest of variables can be determined.

To obtain the optimum operating condition, all the energy consumptions are considered: both the cooling machine compressor and the hydraulic pumping. After that, a global coefficient of performance is defined as the relation of absorbed energy from the cold region and the consumed energy by the compressor and the pump,

$$COP_G = \frac{\dot{Q}_{evap}}{\dot{W}_{comp} + \dot{W}_{pump}} \tag{12}$$

Finally, to different pumping heads, respective COP_G values were obtained. Table 1 shows the calculated values of the main variables at different pumping head values.

Table 1

From Table 1 it can be concluded that increasing the pumping head leads to get a higher efficiency. However, it is important to say that this performance is limited by air saturation, and it is showed in Figure 11, where the efficiency growth is less significant as the pumping head increases. As well as Figure 11, Figure 12 shows the asymptotic performance of the condensation temperature to greater pumping head.

Figure 11

Figure 12

At the same time, as the pumping pressure is higher, obviously, the pumping energy is higher too, but the power consumed by the chiller compressor is reduced because the higher efficiency of the solar roof produces a lower condensation temperature.

Figure 13

Figure 14

Global coefficient of performance (COP_G) is defined as the relation of absorbed energy from the cold region and the consumed energy by the compressor and the pump. It includes and reflects the different trends of energy consumption. Since cooling capacity has been considered constant in this study, maximum COP_G appears when the point of lower energy consumption is reached. In this case, the recommended water pumping head is around 27 m. At this point, the pump energy consumption is 15% and the chiller compressor is 85% of the total.

5. Conclusions

An environmentally friendly alternative to heat dissipation in buildings has been integrated in an air conditioning system and its energy consumption optimisation has been carried out. It has been necessary to include all the elements in a global model. The contradictory effects of the pumping head increment on the Hydrosolar Roof efficiency have been overcome with a CFD simulation. Besides, a cooling machine thermodynamic model has been carried out using EES and the hydraulic network has also been considered.

Increasing the pumping head, and therefore pumping energy consumption, causes a better Hydrosolar Roof efficiency, lower condensing temperature and, as a consequence, less energy is consumed at the cooling machine compressor. This situation with opposite effects is described and calculated for different pumping heads. To reflect the contradictory response of the elements, a global coefficient of performance is defined as the relation of absorbed energy from the cold region and the consumed energy by the compressor and the pump. Using this parameter, the most suitable pumping is calculated.

This paper has showed that Hydrosolar Roofs are a demonstrated alternative to mechanical draught

cooling towers to heat dissipation in buildings. The components and the global system can easily be modelled and optimised for minimum energy consumption.

6. Acknowledgements

The authors wish to acknowledge the collaboration in the calculations of A. Navarro, as well as José María Galán, Energy, Comfort and Environment S.L. manager, as the proposer of the original idea.

7. References

Alam, K.C.A., Saha, B.B., Akisawa, A., Kashiwagi, T., 2001. Optimization of a solar driven adsorption refrigeration system, Energy Conversion and Management. Vol. 42, No 6, pp. 741-753.

ASHRAE. ASHRAE Handbook-Fundamentals; 1997. American Society of Heating, Refrigerating and Air-Conditioning Engineers Inc.

Best, R. and Ortega, N., 1999. Solar refrigeration and cooling, Renewable Energy. Vol. 16, No 1-4, pp. 685-690.

Biancardi, F.R., Sitler, J.W., Melikian, G., 1982. Development and test of solar Rankine cycle heating and cooling systems, International Journal of Refrigeration, Vol. 5, No 6, pp. 351-360.

Braun, J.E. and Doderrich, G.T., 1990. Near-optimal control of cooling towers for chilled-water systems. ASHRAE Trans;96(2):806-13.

Cassidy, M.P. and Stack, J.F., 1988. Applying adjustable speed AC drives to cooling tower fans. In: Annual Petroleum and Chemical Industry Conference. IEEE.

E1296-92: Standard terminology relating to liquid particle statistics. "1996 Annual Book of ASTM Standards, General Methods and Instrumentation, Vol. 14.02" pp. 810-812.

Fisenko, S.P., Brin, A.A., Petruchick, A.I., 2004. Evaporative cooling of water in a mechanical draft cooling tower, International Journal of Heat and Mass Transfer, Vol. 47, pp 165-177.

Florides, G.A., Tassou, S.A., Kalogirou, S.A., Wrobel, L.C., 2002. Review of solar and low energy cooling technologies for buildings, Renewable and Sustainable Energy Reviews, Vol. 6, No 6, pp. 557-572.

Lu, L., Cai, W., Soh, Y.C., Xie, L., Li, S., 2004. HVAC system optimization-condenser water loop, Energy Conversion and Management, Vol. 45, pp. 613-630

Lucas, M., Martínez, P., Sánchez, A., Viedma, A., Zamora, B., 2003. Improved Hydrosolar Roof for buildings' air conditioning, Energy and Buildings, Vol. 35, No 9, pp. 963-970.

Merkel, F., 1926. Evaporative Cooling, Zeits, Verein Deutscher Ingenieure 70, pp. 120-128.

Mohiuddin, A. K. M. and Kant, K., 1996. Knowledge base for the systematic design of wet

cooling towers, I. J. Refrig, Vol. 19, No. 1, pp. 43-51.

Nottage, H. B., 1941. Merkel´s cooling diagram as a performance correlation for air water evaporative cooling system, ASHVE Trans. 47, 429.

Papadopoulos, A.M., Oxizidis, S., Kyriakis, N., 2003. Perspectives of solar cooling in view of the developments in the air-conditioning sector, Renewable and Sustainable Energy Reviews. Vol. 7, No 5, pp. 419-438.

Rapin, P.J. and Jaquard, P., 1997. Installations Frigorifiques, PYC-Edition, Paris. ISBN:2-85330-119-2.

Sánchez, A. and Viedma, A., 2001. Hydrosolar roof for integrated energy dissipation and capture in buildings, Energy and Buildings, Vol. 33, No 7, pp. 673-682.

Sánchez, M.M., Lucas, M., Martínez, P., Sánchez, A. and Viedma, A., 2002. Climatic solar roof: an ecological alternative to heat dissipation in buildings, Solar Energy, Vol. 73, No 6, pp. 419-432.

Sözen, A., Altparmak, D., Usta, H., 2002. Development and testing of a prototype of absorption heat pump system operated by solar energy, Applied Thermal Engineering. Vol. 22, No 16, pp. 1847-1859.

Soymelez, M.S., 2004. On the optimum performance of forced draft counter flow cooling towers, Energy Conversion and Management, In press

Sumathy, K., Yeung, K.H., Yong, L., 2003. Technology development in the solar adsorption refrigeration systems, Progress in Energy and Combustion Science, Vol. 29, No 4, pp. 301-327.

Tillner-Roth, R. and Baehr, H.D., 1994. An International Standard Formulation for the Thermodynamic Properties of 1,1,1,2-Tetrafluoroethane (HFC-134a) for Temperatures from 170 K to 455 K and Pressures up to 70 MPa, J. Phys. Chem, Ref. Data, Vol. 23, No. 5.

H (m)	10.00	14.44	18.89	23.33	27.78	32.22	36.67	41.11	45.56	50.00
VMD (μm)	710.60	578.20	503.80	454.30	418.10	390.10	367.60	349.00	333.20	319.60
$P(10^5$ Pa)	0.68	1.11	1.54	1.97	2.40	2.83	3.26	3.69	4.12	4.55
$\dot{m}_w$ (kg/s)	0.90	1.15	1.36	1.53	1.69	1.84	1.97	2.10	2.22	2.33
W_{pump} (kW)	0.10	0.19	0.30	0.41	0.54	0.68	0.83	0.99	1.17	1.34
η	0.33	0.40	0.45	0.50	0.54	0.57	0.60	0.63	0.66	0.69
T_{sw} (ºC)	42.22	35.97	33.20	31.64	30.63	29.92	29.40	28.99	28.67	28.40
ΔT_{max} (ºC)	16.62	10.37	7.60	6.04	5.03	4.32	3.80	3.39	3.07	2.80
ΔT (ºC)	5.50	4.14	3.44	3.00	2.70	2.47	2.30	2.15	2.03	1.93
T_{dw} (ºC)	36.72	31.83	29.76	28.64	27.93	27.45	27.10	26.84	26.64	26.47
T_{cond} (ºC)	47.22	40.97	38.20	36.64	35.63	34.92	34.40	33.99	33.67	33.40
COP	3.42	4.11	4.61	4.93	5.16	5.34	5.47	5.57	5.66	5.73
Q_{cond}(kW)	20.68	19.89	19.47	19.24	19.10	19.00	18.93	18.87	18.83	18.79
W_{comp} (kW)	4.68	3.89	3.48	3.24	3.10	3.00	2.93	2.87	2.83	2.79
W_{Total} (kW)	4.78	4.08	3.77	3.66	3.64	3.68	3.76	3.87	3.99	4.14
COP_G	3.34	3.92	4.24	4.38	4.40	4.35	4.25	4.14	4.01	3.87

Table 1. System variables and global coefficient of performance for different pumping head values

FIGURE CAPTIONS

Figure 1: Air conditioning system scheme

Figure 2: Cooling machine's Coefficient of Performance as a function of sprayed water temperature for a constant evaporation temperature (4.5ºC)

Figure 3: Hydraulic performance curve

Figure 4: Influence of pressure in water drop size in terms of Volume Median Diameter, *VMD*.

Figure 5: Water temperature evolution (K)

Figure 6: Water vapour mass fraction (kg water/kg air)

Figure 7: Variation of Hydrosolar Roof efficiency as a function of drop size and ΔT_{max}, for $\left(\dot{m}_w/\dot{m}_a\right)$=1

Figure 8: Variation of Hydrosolar Roof efficiency as a function of drop size and water mass flow ratio, for ΔT_{max} = 5ºC

Figure 9: Experimental and numerical efficiency comparison vs. ΔT_{max} (*VMD* = 600 μm)

Figure 10: Experimental and numerical efficiency comparison vs. $\left(\dot{m}_w/\dot{m}_a\right)$ (*VMD* = 600 μm)

Figure 11: Hydrosolar Roof efficiency as a function of pumping head

Figure 12: Condensation temperature evolution for different pumping heads

Figure 13: Energy consumptions as a function of pumping head

Figure 14: Global COP evolution for different pumping heads

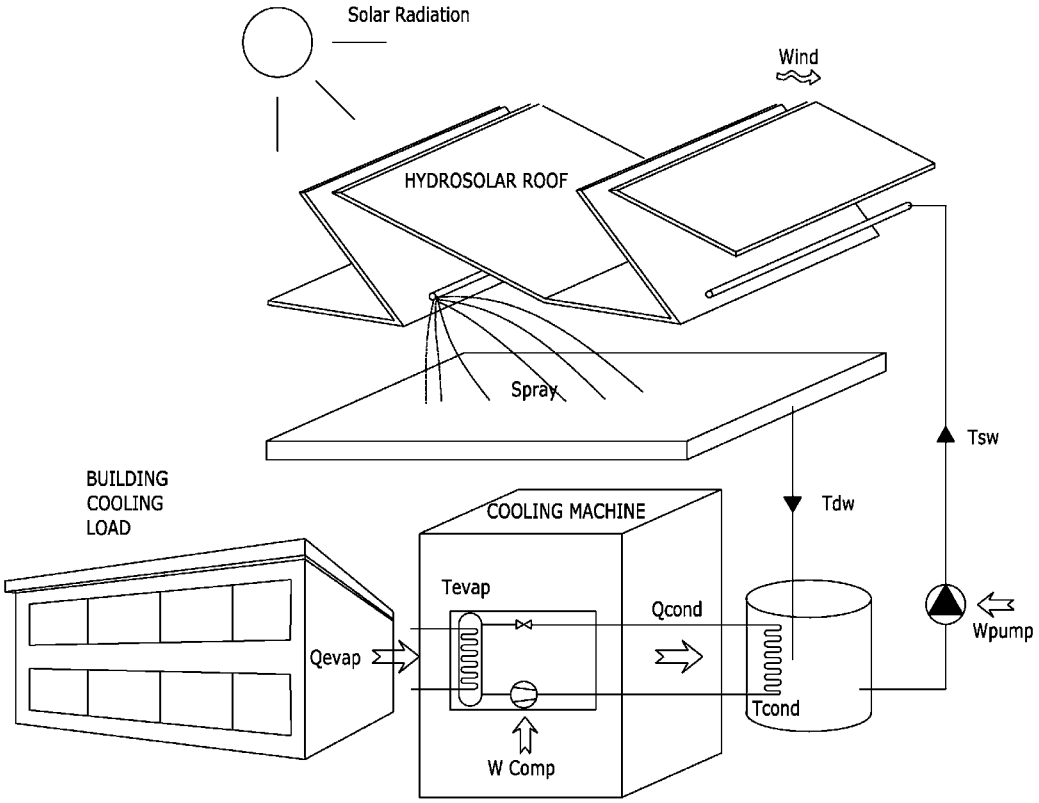

Figure 1: Air conditioning system scheme

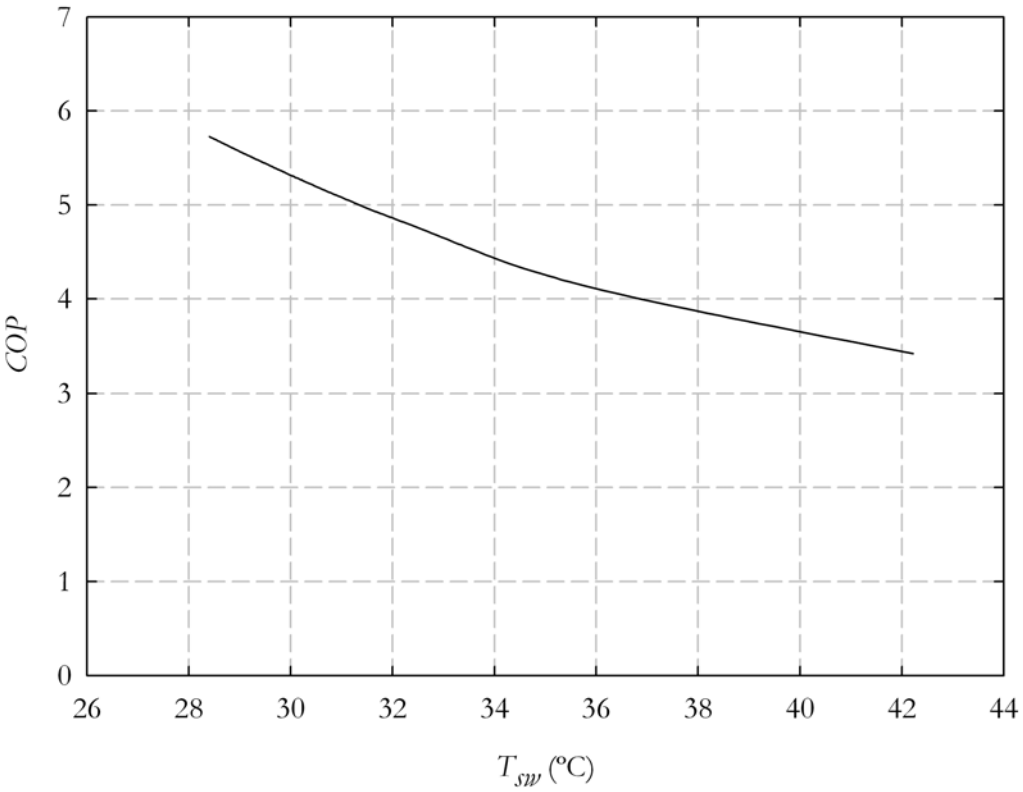

Figure 2: Cooling machine's Coefficient of Performance as a function of sprayed water temperature for a constant evaporation temperature (4.5ºC)

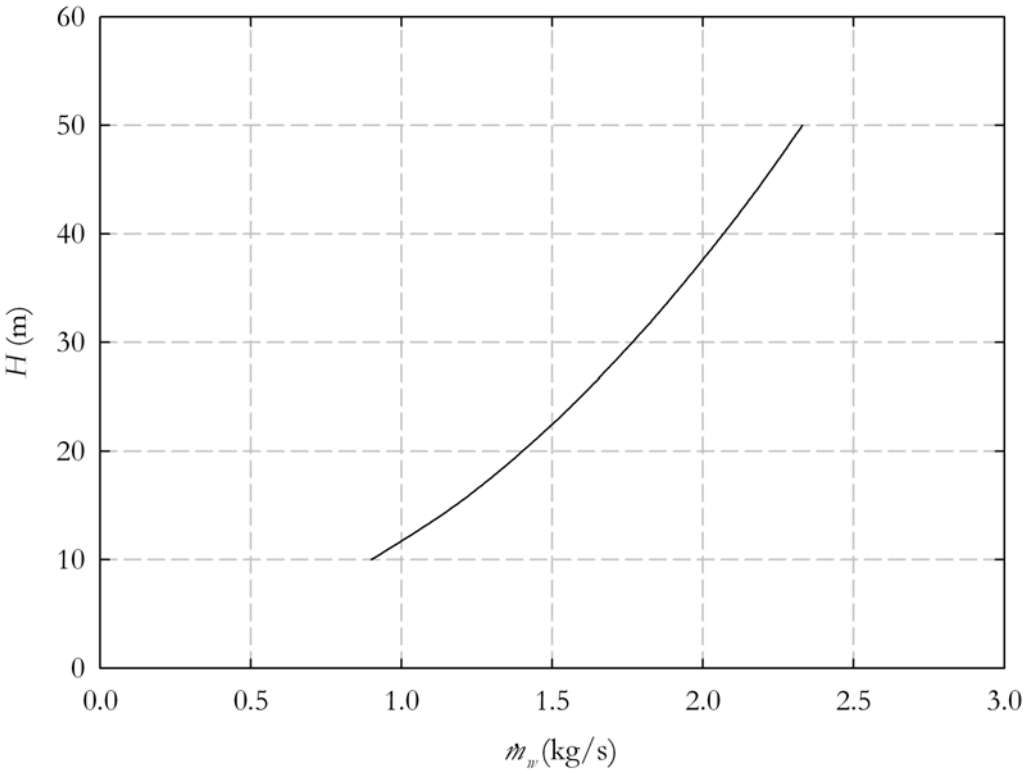

Figure 3: Hydraulic performance curve

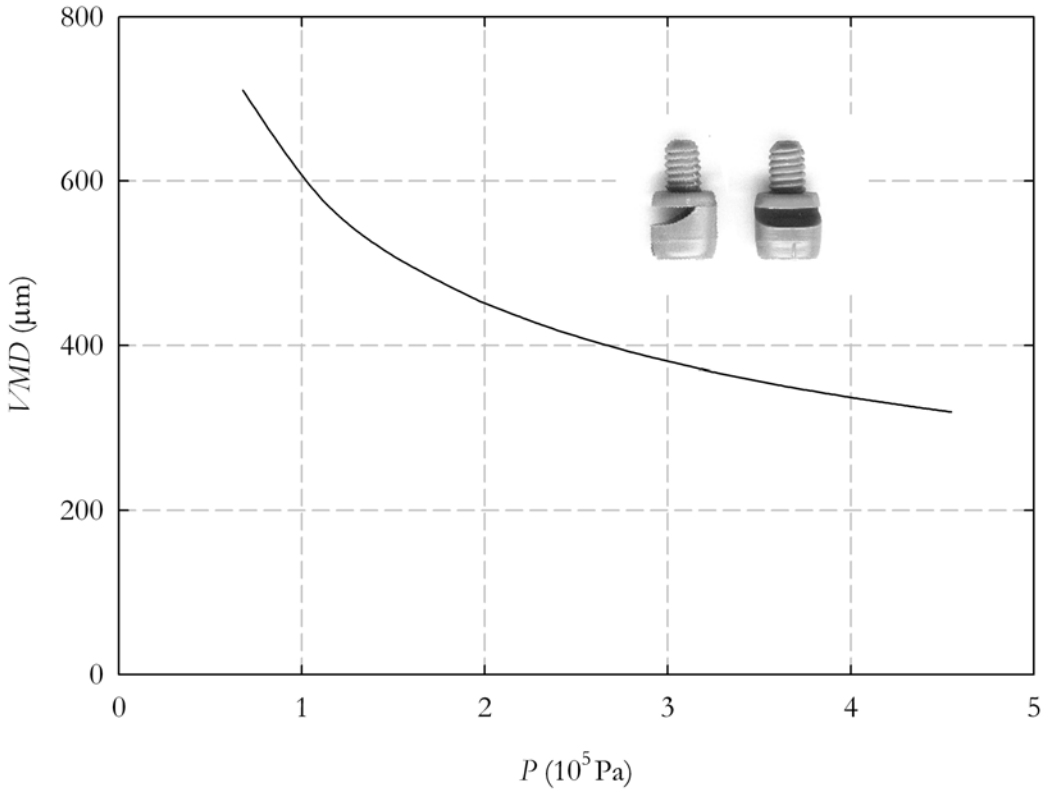

Figure 4: Influence of pressure in water drop size in terms of Volume Median Diameter, VMD.

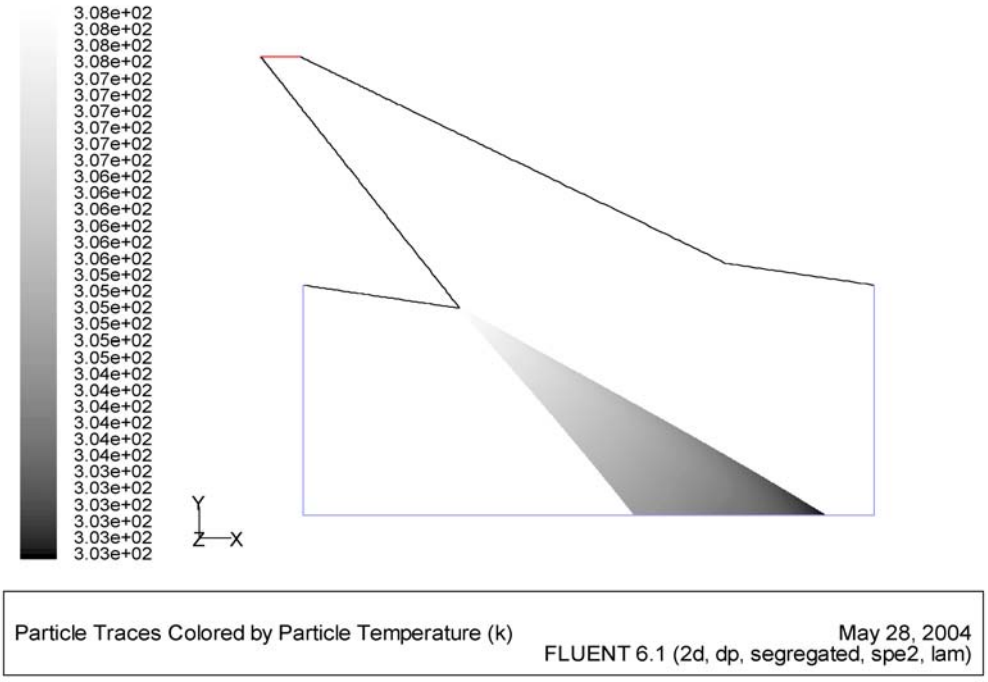

Figure 5: Water temperature evolution (K)

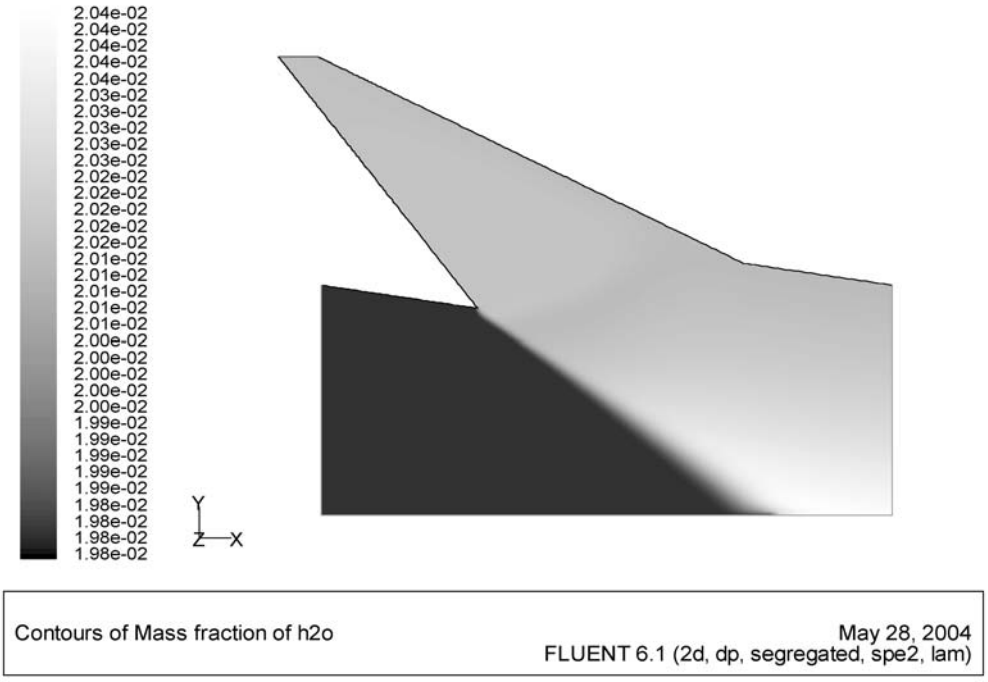

Figure 6: Water vapour mass fraction (kg water/kg air)

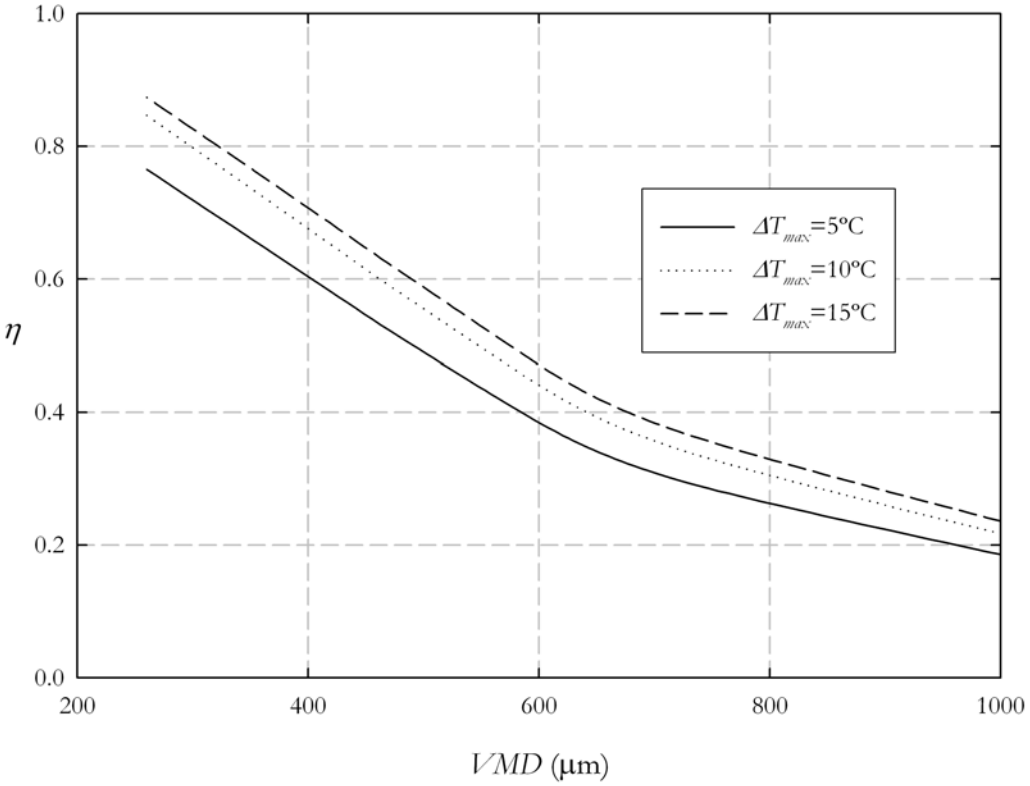

Figure 7: Variation of Hydrosolar Roof efficiency as a function of drop size and ΔT_{max}, for $(\dot{m}_w/\dot{m}_a)$=1

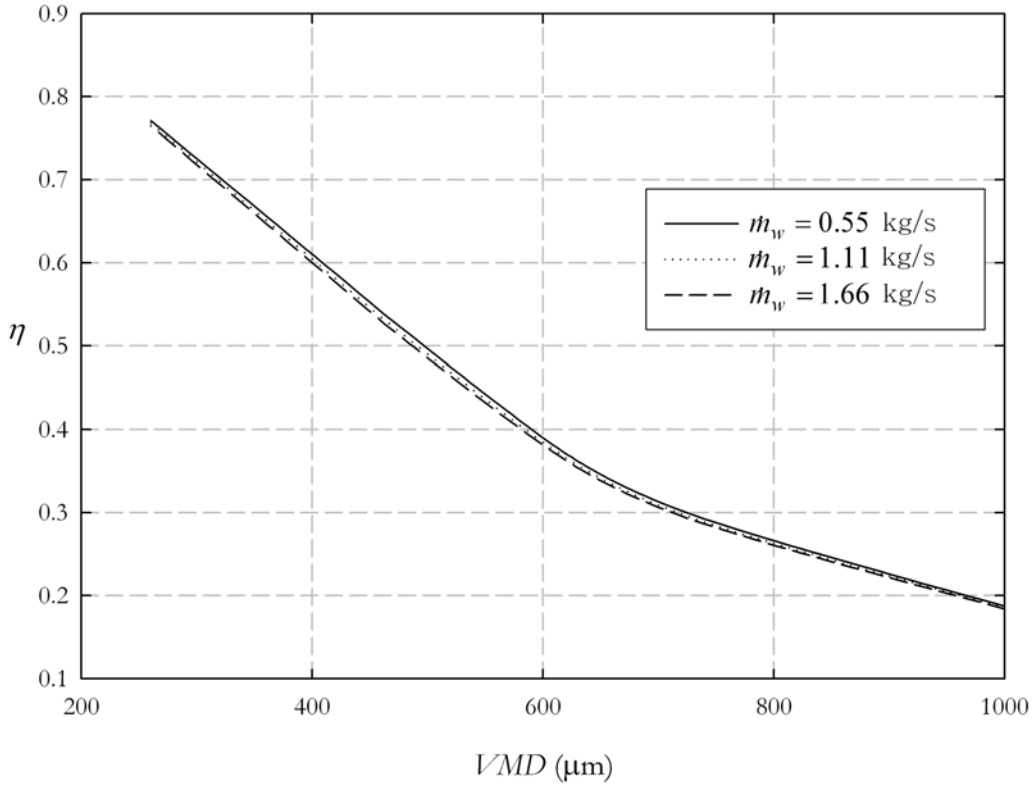

Figure 8: Variation of Hydrosolar Roof efficiency as a function of drop size and water mass flow ratio, for ΔT_{max} = 5ºC

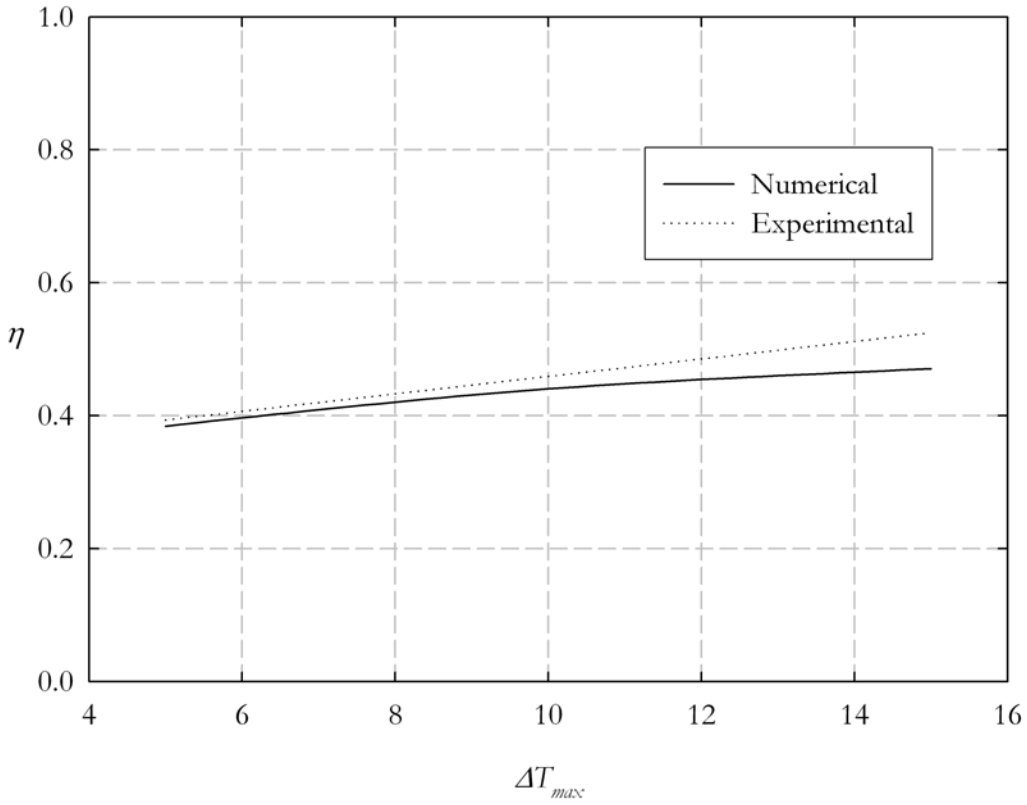

Figure 9: Experimental and numerical efficiency comparison vs. ΔT_{max} (VMD = 600 μm)

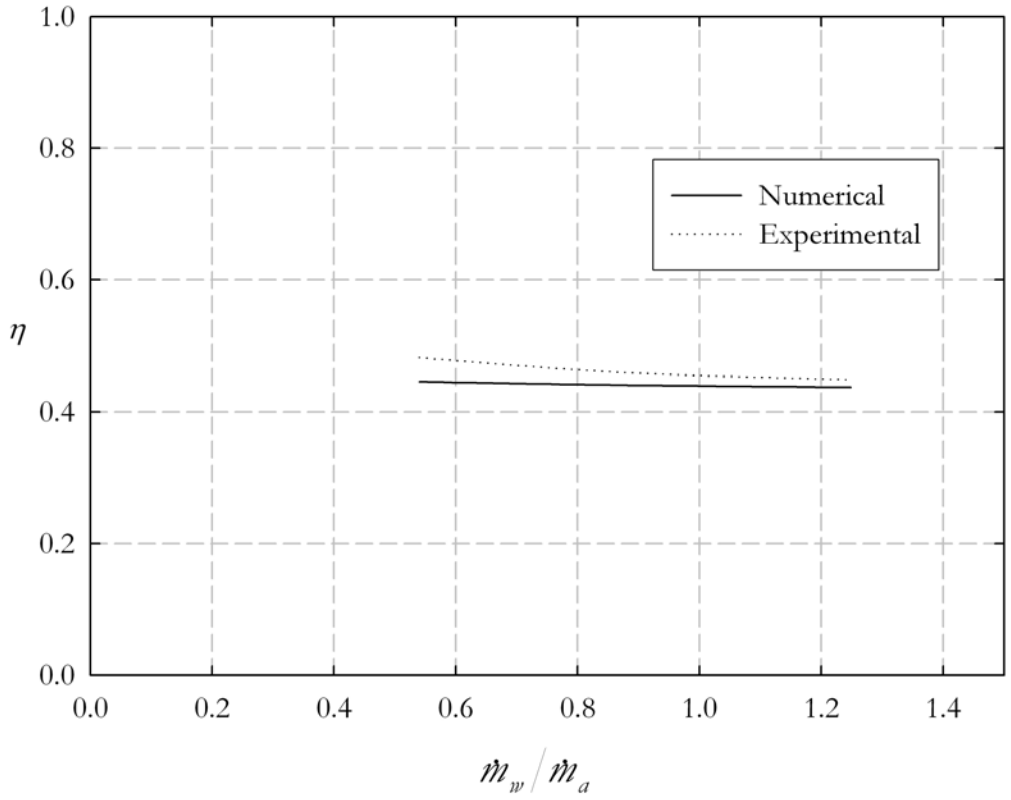

Figure 10: Experimental and numerical efficiency comparison vs. $(\dot{m}_w/\dot{m}_a)$ (VMD = 600 μm)

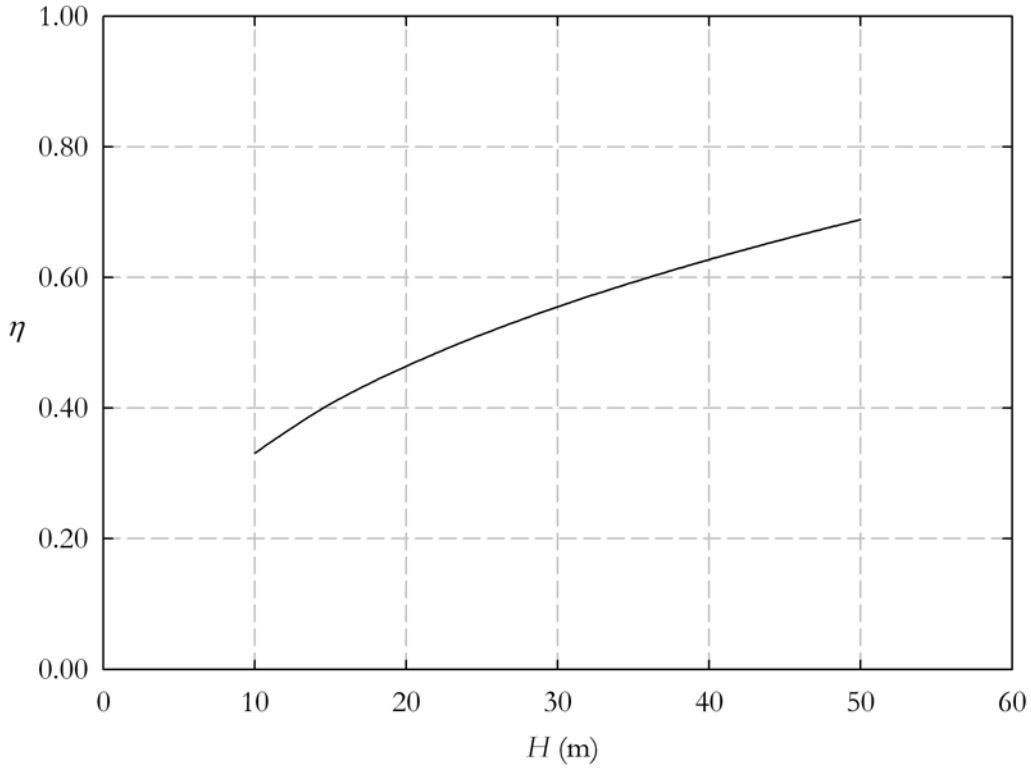

Figure 11: Hydrosolar Roof efficiency as a function of pumping head

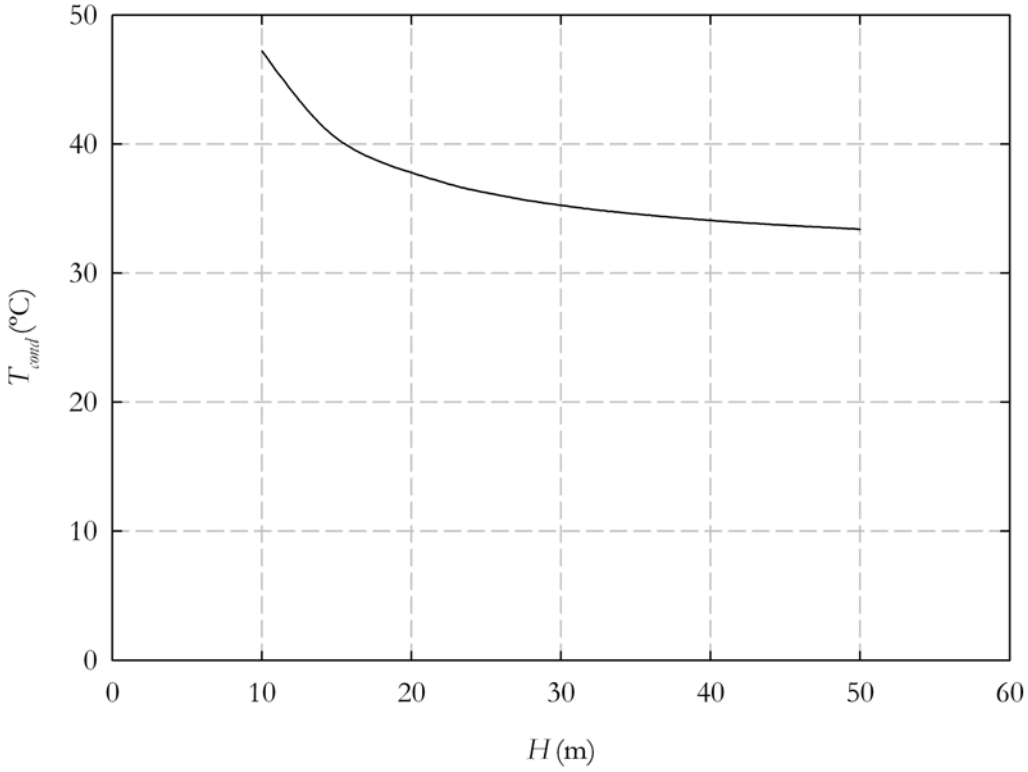

Figure 12: Condensation temperature evolution for different pumping heads

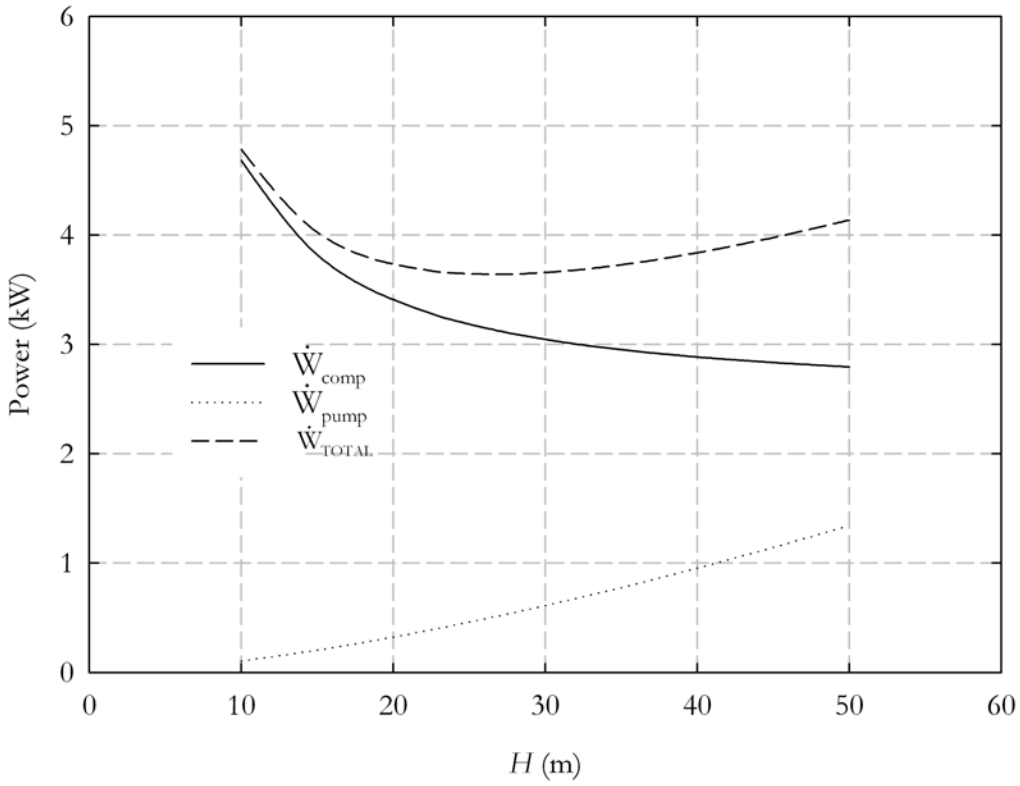

Figure 13: Energy consumptions as a function of pumping head

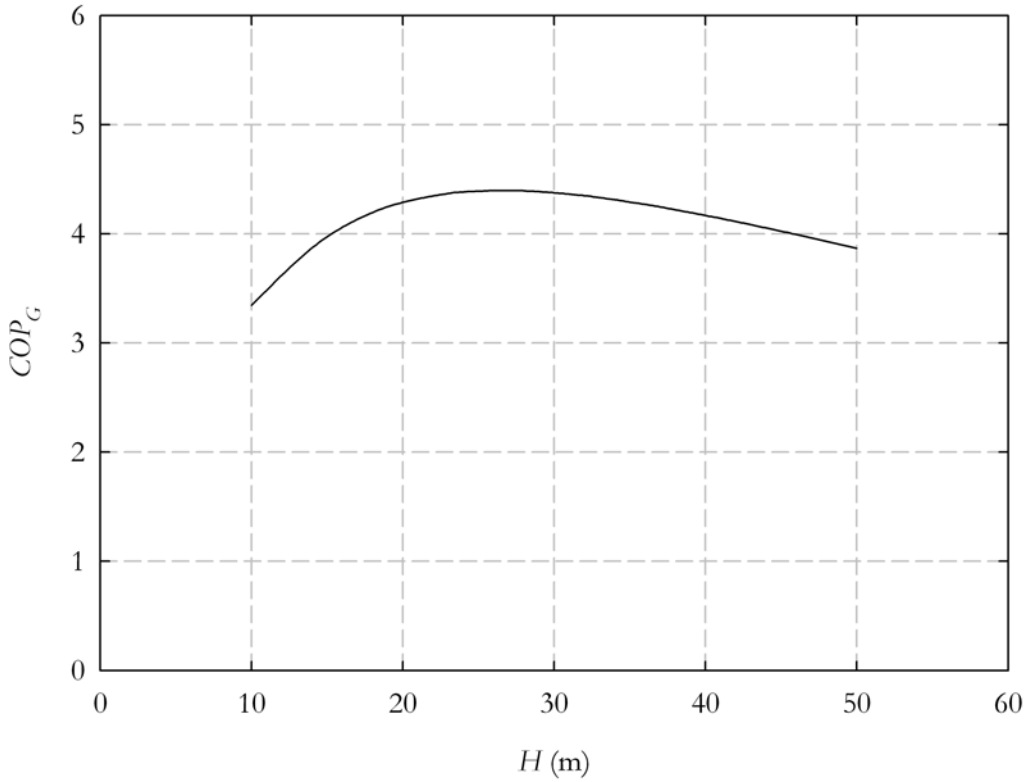

Figure 14: Global COP evolution for different pumping heads